The X/Gamma-ray Imaging Spectrometer (XGIS) for THESEUS and other mission opportunities

Amati, Lorenzo; Labanti, Claudio; Mereghetti, Sandro; Frontera, Filippo; Campana, Riccardo; Auricchio, Natalia; Baldazzi, Giuseppe; Bellutti, Pierluigi; Bertuccio, Giuseppe; Branchesi, Marica

Total number of authors:
64

Published in:
Proceedings of SPIE

Link to article, DOI:
10.1117/12.2630178

Publication date:
2022

Document Version
Publisher's PDF, also known as Version of record

PROCEEDINGS OF SPIE

SPIEDigitalLibrary.org/conference-proceedings-of-spie

The X/Gamma-ray Imaging Spectrometer (XGIS) for THESEUS and other mission opportunities

Lorenzo Amati, Claudio Labanti, Sandro Mereghetti, Filippo Frontera, Riccardo Campana, et al.

Lorenzo Amati, Claudio Labanti, Sandro Mereghetti, Filippo Frontera, Riccardo Campana, Natalia Auricchio, Giuseppe Baldazzi, Pierluigi Bellutti, Giuseppe Bertuccio, Marica Branchesi, Reginald C. Butler, Maria D. Caballero-Garcia, Anna E. Camisasca, Alberto J. Castro-Tirado, Leo Cavazzini, Riccardo Ciolfi, Adriano De Rosa, Federico Evangelisti, Ruben Farinelli, Lisa Ferro, Francesco Ficorella, Mauro Fiorini, Fabio Fuschino, José L. Gasent-Blesa, Giancarlo Ghirlanda, Marco Grassi, Cristiano Guidorzi, Paul Hedderman, Irfan Kuvvetli, Giovanni La Rosa, Paolo Lorenzi, Piero Malcovati, Ezequiel Marchesini, Martino Marisaldi, Michele Melchiorri, Filippo Mele, Malgorzata Mikhalska, Mauro Orlandini, Piotr Orleanski, Soren Moller Pedersen, Raffaele Piazzolla, Alexandre Rachevski, Irina Rashevskaya, Piero Rosati, Victor Reglero, Samuele Ronchini, Andrea Santangelo, Ruben Salvaterra, Paolo Sarra, Francesca Sortino, Giuseppe Sottile, Giulia Stratta, Stefano Squerzanti, John B. Stephen, Chris Tenzer, Luca Terenzi, Alessio Trois, Andrea Vacchi, Enrico Virgilli, Angela Volpe, Marek Winkler, Gianluigi Zampa, Nicola Zampa, Andrzej Zdziarski, "The X/Gamma-ray Imaging Spectrometer (XGIS) for THESEUS and other mission opportunities," Proc. SPIE 12181, Space Telescopes and Instrumentation 2022: Ultraviolet to Gamma Ray, 1218126 (31 August 2022); doi: 10.1117/12.2630178

SPIE.

Event: SPIE Astronomical Telescopes + Instrumentation, 2022, Montréal, Québec, Canada

The X/Gamma-ray Imaging Spectrometer (XGIS) for THESEUS and other mission opportunities

Lorenzo Amati[*a], Claudio Labanti[a], Sandro Mereghetti[b], Filippo Frontera[c,a], Riccardo Campana[a], Natalia Auricchio[a], Giuseppe Baldazzi[d], Pierluigi Bellutti[e], Giuseppe Bertuccio[f], Marica Branchesi[g], Reginald C. Butler[a], Maria D. Caballero-Garcia[h], Anna E. Camisasca[c], Alberto J. Castro-Tirado[h], Leo Cavazzini[c], Riccardo Ciolfi[i], Adriano De Rosa[a], Federico Evangelisti[j], Ruben Farinelli[a], Lisa Ferro[c], Francesco Ficorella[e], Mauro Fiorini[b], Fabio Fuschino[a], José L. Gasent-Blesa[k], Giancarlo Ghirlanda[l], Marco Grassi[m], Cristiano Guidorzi[c], Paul Hedderman[n], Irfan Kuvvetli[o], Giovanni La Rosa[p], Paolo Lorenzi[q], Piero Malcovati[m], Ezequiel Marchesini[a], Martino Marisaldi[r], Michele Melchiorri[j], Filippo Mele[f], Malgorzata Michalska[s], Mauro Orlandini[a], Piotr Orleanski[s], Soren Moller Pedersen[o], Raffaele Piazzolla[t], Alexandre Rachevski[u], Irina Rashevskaya[u], Piero Rosati[c], Victor Reglero[k], Samuele Ronchini[g], Andrea Santangelo[n], Ruben Salvaterra[b], Paolo Sarra[q], Francesca Sortino[l], Giuseppe Sottile[p], Giulia Stratta[t], Stefano Squerzanti[j], John B. Stephen[a], Chris Tenzer[n], Luca Terenzi[a], Alessio Trois[v], Andrea Vacchi[w], Enrico Virgilli[a], Angela Volpe[y], Marek Winkler[s], Gianluigi Zampa[u], Nicola Zampa[u], Andrzej Zdziarski[x]

[a]INAF – OAS Bologna, via P. Gobetti 93/3, 40129 Bologna (BO), Italy; [b]INAF – IASF Milano, via A. Corti 12, I-20133 Milano, Italy; [c]Università degli Studi di Ferrara - Dipartimento di Fisica e Scienze della Terra, Via Saragat 1, I-44122 Ferrara, Italy; [d]Università degli studi di Bologna – Dipartimento di Fisica e Astronomia, viale Berti Pichat 6/2
40127 Bologna – Italy; [e]Fondazione Bruno Kessler (FBK), Via Sommarive, 18, 38123, Povo, Italy; [f]Politecnico di Milano, Via Anzani, 42, I-22100, Como, Italy; [g]Gran Sasso Science Institute, Viale Francesco Crispi, 7, 67100 L'Aquila – Italy; [h]Instituto de Astrofísica de Andalucía, Gta. de la Astronomía, s/n, 18008 Granada, Spain; [i]INAF – Osservatorio Astronomico di Padova, Vicolo Osservatorio 5 - 35122 – Padova, Italy; [J]INFN – Sezione di Ferrara, Via Saragat, 1
44122 Ferrara, Italy; [k]Image Processing Laboratory, University of Valencia, c/ Catedrático José Beltrán, 2, E46980, Paterna (Valencia), Spain; [l]INAF – Osservatorio Astronomico di Brera, via Brera 28, 20121 Milano – Italy; [m]University of Pavia, Via Ferrata, 5, I-27100 Pavia, Italy; [n]Institute of Astronomy and Astrophysics – University of Tübingen, Sand 1, D-72076 Tübingen, Germany; [o]DTU Space, National Space Institute, Technical University of Denmark, Kgs. Lyngby, Denmark; [p]INAF – IASF Palermo, Area della Ricerca CNR, via Ugo La Malfa 153, Palermo, Italy; [q]OHB – Italia, Via Gallarate, 150, 20151 Milano, Italy; [r]Department of Physics and Technology – University of Bergen, Allégaten 55,
5007 Bergen, Norway; [s]Centrum Badań Kosmicznych PAN, ul. Bartycka 18a, 00-716 Warszawa, Poland; [t]INAF – IAPS Roma, via Fosso del Cavaliere 100, 00133 Roma RM; [u]INFN, Sezione di Trieste, Località Padriciano, 99, I-34149, Trieste, Italy; [v]INAF – Osservatorio Astronomico di Cagliari, Via della Scienza n. 5
09047 Selargius (CA), Italy; [w]University of Udine, Via delle Scienze, 206, I-33100, Udine, Italy; [y]Italian Space Agency, Via del Politecnico, I-00133, Rome, Italy; [x]Nicolaus Copernicus Astronomical Center, Polish Academy of Sciences, Bartycka 18, PL-00-716 Warszawa, Poland.

[*] lorenzo.amati@inaf.it; phone +39 339 5991640; fax +39 051 6398723

Space Telescopes and Instrumentation 2022: Ultraviolet to Gamma Ray, edited by Jan-Willem A. den Herder, Shouleh Nikzad, Kazuhiro Nakazawa, Proc. of SPIE Vol. 12181, 1218126 · © 2022 SPIE · 0277-786X · doi: 10.1117/12.2630178

ABSTRACT

We describe the science case, design and expected performances of the X/Gamma-ray Imaging Spectrometer (XGIS), a GRB and transients monitor developed and studied for the THESEUS mission project, capable of covering an exceptionally wide energy band (2 keV – 10 MeV), with imaging capabilities and location accuracy <15 arcmin up to 150 keV over a Field of View of 2sr, a few hundreds eV energy resolution in the X-ray band (<30 keV) and few micro seconds time resolution over the whole energy band. Thanks to a design based on a modular approach, the XGIS can be easily re-scaled and adapted for fitting the available resources and specific scientific objectives of future high-energy astrophysics missions, and especially those aimed at fully exploiting GRBs and high-energy transients for multi-messenger astrophysics and fundamental physics.

Keywords: High-energy astrophysics: future missions; Gamma-ray:bursts; Time-domain astronomy; Multi-messenger astrophysics; Space astrophysics: X and gamma-ray detectors; X-rays: transients.

1. INTRODUCTION

The Transient High-Energy Sky and Early Universe Surveyor (THESEUS) mission concept[1-3] aims at fully exploiting Gamma-Ray Bursts (GRB) for early Universe and multi-messenger astrophysics, as well as providing a substantial advance in time-domain astronomy through detection, accurate location, multi-wavelength (0.3 keV – 10 MeV plus near IR) characterization, and redshift measurement, of many classes of high-energy transients[4-9]. Developed by a large international collaboration, in 2018 THESEUS was selected by ESA for a three years Phase 0/A study as one of the three candidates for the M5 medium-class space mission opportunity for a launch in ~2032[3].

The scientific goals for the exploration of the early Universe[4] require the detection, identification, and characterization of several tens of long GRBs occurred in the first billion years of the Universe ($z > 6$) within the 4 years of nominal mission lifetime of THESEUS. This would be a giant leap with respect to what has been obtained in the last 20 years (7 GRBs at > 6), using past and current GRB dedicated experiments like Swift/BAT, Fermi/GBM, Konus-WIND combined with intensive follow-up programs from the ground with small robotic and large telescopes (e.g., VLT). This breakthrough performance can be achieved by overcoming the current limitations through an extension of the GRB monitoring passband to the soft X-rays with an increase of at least one order of magnitude in sensitivity with respect to previously flown wide-field X-ray monitors, as well as a substantial improvement of the efficiency of counterpart detection, spectroscopy and redshift measurement through prompt on-board NIR follow-up observations. At the same time, the objectives on multi-messenger astrophysics[5-6] and, more generally, time domain astronomy[7-9] and synergies with future very large facilities[10-11], require: a) a substantial advancement in the detection and localization, over a large (> 2 sr) Field-of-View (FoV) of short GRBs as electromagnetic counterparts of GW signals coming from NS-NS, and possibly NS-BH) mergers; b) monitoring the high-energy sky with an unprecedented combination of sensitivity, location accuracy and field of view in the soft X-rays; c) imaging up to the hard X-rays and spectroscopy / timing to the soft gamma-rays.

Based on these scientific requirements and the unique heritage and Consortium worldwide leadership in the enabling technologies, the THESEUS payload would include the following scientific instruments[2,3]:

- **Soft X-ray Imager (SXI, 0.3 – 5 keV):** a set of two "Lobster-eye" telescope units, covering a total FoV of ~0.5 sr with source location accuracy ≤2', focusing onto innovative large size X-ray CMOS detectors[12];
- **X/Gamma-ray Imaging Spectrometer (XGIS, 2 keV – 10 MeV**): a set of two coded-mask cameras using monolithic SDD+CsI X- and gamma-ray detectors, granting a ~2 sr imaging FoV and a source location accuracy <15 arcmin in 2-150 keV and few □s timing resolution[13];
- **InfraRed Telescope (IRT, 0.7 – 1.8 μm**): a 0.7-m class IR telescope with 15'x15' FoV, with imaging (I, Z, Y, J and H) and moderate spectroscopic (resolving power, R~400, through 2'x2' grism) capabilities[14].

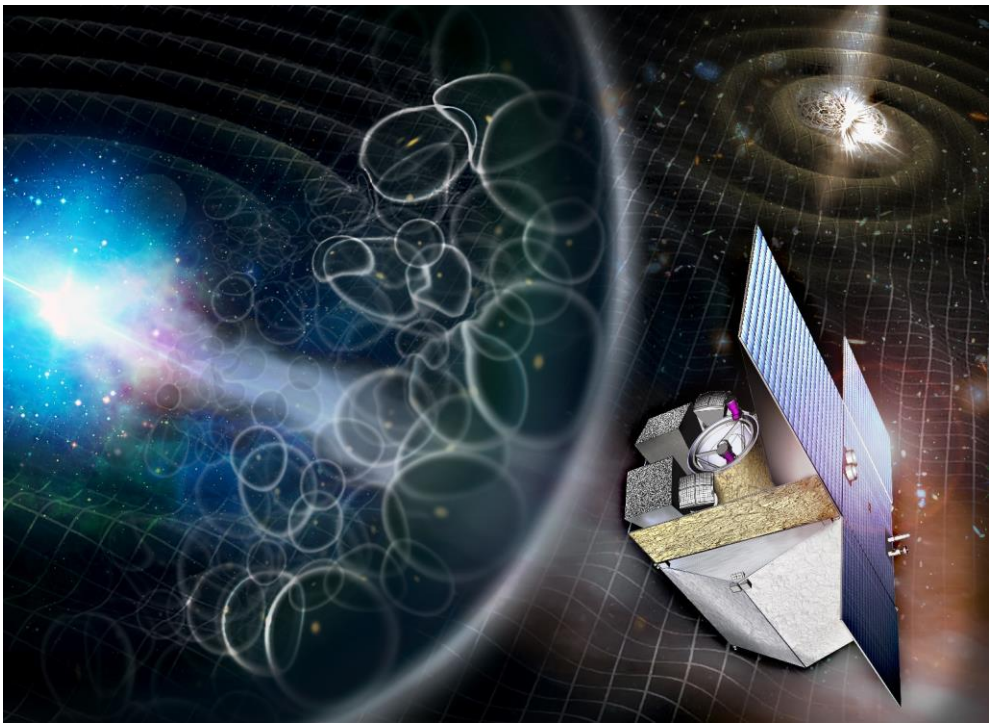

Figure 1. A pictoric view of the main subjects of investigations of THESEUS and, on the bottom-right part, a sketch of the spaceraft design and payload accommodation as investigated during ESA/M5 Phase 0/A study (credits: ESA THESEUS Assessment Study report: https://sci.esa.int/web/cosmic-vision/-/theseus-assessment-study-report-yellow-book).

Figure 1 shows a pictoric view of the main subjects of investigations of THESEUS and a sketch of the spaceraft design and payload accommodation as assessed during ESA/M5 Phase 0/A study. The baseline launcher / orbit configuration is a launch with Vega-C to a low inclination (<6°) Low Earth Orbit (LEO, 550-640 km altitude), which has the unique advantages of granting a low and stable background level in the high-energy instruments, allowing the exploitation of the Earth's magnetic field for spacecraft fast slewing and facilitating the prompt transmission of transient triggers and positions to the ground. The mission profile will include a spacecraft autonomous *slewing capability >7°/min*, allowing fast NIR follow-up with the IRT of GRBs and transients detected and localized by the monitors (SXI and XGIS).

In this article we describe the concept of the THESEUS X/Gamma-ray Imaging Spectrometer (XGIS)[13], a GRB and transients monitor capable of covering an exceptionally wide energy band (2 keV – 10 MeV), with imaging capabilities and location accuracy <15 arcmin up to 150 keV over a Field of View of 2sr, a few hundred eV energy resolution in the X-ray band (<30 keV) and few micro seconds time resolution over the whole energy band. This unprecedented capabilities are obtained through a coded mask imaging system joined to an innovative detection plane made of pixels built of Silicon Driift Detectors (SDD, 2- 30 keV) coupled to CsI crystal scintillator detectors (20 keV - 10 MeV). In synergy with the Soft-X-ray Imager (0.3 – 5 keV) and the Infra-Red Telescope (IRT), combined with spacecraft fast slewing capabilities, the XGIS will allow THESEUS to detect, accurately localize and characterize any class of GRBs (long, short, high-z, sub-energetic, ultra-long, etc.), as well as further bright X/gamma-ray transients, for a fraction of which the IRT will provide detection, arcsec localization, moderate spectroscopy and on-board redshift determination.

Thanks to its capability of detecting, localizing and characterizing any kind of GRBs (short, long, X-Ray Flashes, under-luminous, ultra-long) and a design based on a modularity approach, the XGIS can be easily re-scaled and adapted for fitting the available resources and specific scientific objectvies of other high-energy astrophysics missions. Moreover, an XGIS-like instrument will provide an important contribution also to the high-z GRB detection and localization, thus

enabling GRB cosmology. The ESA Phase A study of THESEUS (2018-2021) and related TDAs grants an already good TRL level (e.g., detection module prototype, SDD detectors and specifically designed ASIC already under testing).

2. SCIENTIFIC MOTIVATION AND REQUIREMENTS FOR THE XGIS

The inclusion in the THESUS payload of a broad field of view hard X/soft gamma-ray detection system, covering a >2sr FoV (that includes that of the SXI) and extending the energy band from few keV up to several MeV with at least a few hundred cm^2 effective area over the whole range is fundamental for:

a) detecting and localizing short GRBs, which are a key phenomenon for multi-messenger astrophysics, being up to now the most likely and only one detected EM counterparts of GW signals (specifically, from NS-NS and NS-BH mergers), and determining the hard spectrum of these events, which makes them mostly undetectable with the SXI;

b) complementing the SXI capabilities for the detection and localization of high-z GRBs, thanks to the large effective area at <10 keV with respect to past/current GRB detectors;

c) providing unique clues to the physics and geometry of the emission of GRBs and other bright X-ray transients through sensitive timing and spectroscopy over an unprecedentedly wide energy band;

d) detecting possible absorption features in the low-energy spectra of GRBs that may be used for investigating the circum-burst environment, and hence the nature of the progenitor star, as well as inferring the redshift;

e) allowing accurate spectral and timing characterization of GRB prompt emission over four orders of magnitude, thus further extending THESEUS scientific return by enabling tests of fundamental physics (e.g., Lorentz Invariance Violation) and the use of GRBs for measuring cosmological parameters (through spectrum-energy correlations).

Table 1. Summary of main scientific requirements for THESEUS scientific instruments.

SXI sensitivity (3σ)	1.8×10^{-11} erg/cm^2/s (0.3-5 keV, 1500 s)
	10^{-10} erg/cm^2/s (0.3-5 keV, 100 s)
XGIS sensitivity (1s, 3σ)	10^{-8} erg/cm^2/s (2-30 keV)
	3×10^{-8} erg/cm^2/s (30-150 keV)
	2.7×10^{-7} erg/cm^2/s (150 keV-1 MeV)
IRT sensitivity (imaging, SNR=5, 150 s)	20.9 (I), 20.7 (Z), 20.4 (Y), 20.7 (J), 20.8 (H)
SXI field-of-view	0.5 sr - 31x61 degrees^2
XGIS field-of-view (area corresponding to >20% efficiency)	2 sr (2-150 keV) – 117x77 degrees^2
	4 sr (≥150 keV)
IRT field-of-view	15'x15'
Redshift accuracy (6≤z≤10)	≤10%
IRT resolving power	≥400
XGIS background stability	≤10% (over 10 minutes)
SXI positional accuracy (0.3-5 keV, 99% c.l.)	≤2 arcminutes
XGIS positional accuracy (2-150 keV, 90% c.l.)	≤7 arcminutes (50% of the triggered sGRB)
	≤15 arcminutes (90% of the triggered sGRB)
IRT positional accuracy (5σ detections)	≤5 arcsecond (real-time)
	≤1 arcsecond (post-processing)

In addition, as the SXI lobster-eye telescopes can be triggered by several classes of transient phenomena (e.g., flare stars, X-ray bursts, etc), the detection in hard X-rays with the XGIS provides an efficient tool of identifying bona fide GRBs.

The core science requirements of THESEUS have been assessed by simulating a number of observational scenarios during the ESA/M5 assessment phase 0/A study. The main goal of these simulations was to ensure that a set of observation strategies exists enabling the core scientific requirements of THESEUS. These were then injected in the industrial study for their further validation and optimization. The simulations made use of a state-of-the-art GRB population model based on the original work by THESEUS team members[8].

An overall summary of the main scientific requirements for THESEUS scientific instruments, and specifically for the XGIS, is reported in Table 1.

3. XGIS INSTRUMENT DESCRIPTION

The architecture of the XGIS system consists of two X/gamma-ray cameras (Figure 2), two power supply units (XSU), a Data Handling Unit (DHU) and harness[13,15-18]. Each XGIS camera is powered from its dedicated XSU and is directly connected to the DHU. DHU is the interface of XGIS with the S/C for commands, data downloading and power that is then delivered to the XSUs. The burst trigger functionality is part of the SW of the DHU, which includes also the mass memory and operates as instrument control unit (ICU).
XGIS has imaging capabilities up to 150 keV, with a FoV larger than and fully overlapping with the SXI one, and has spectrometric capabilities covering a wide energy range from few keV to several MeV, partially overlapping the SXI one in the soft X-rays.

As an imager, XGIS is based on the *coded mask* principle, with the mask *shadowgram* being recorded by a position sensitive detector, that can then be deconvolved into a sky image. A XGIS camera has a partially-coded imaging FoV of 77×77 degrees^2; the two cameras are misaligned by ±20° with respect to SXI and IRT, thus providing a total FoV of 117×77 degrees^2. The size of the point spread function in the sky image is determined by the ratio of the mask pixel size and the mask-to-detector distance. Above 150 keV, the mask and the collimator of a XGIS camera become transparent, thus imaging capabilities are lost and FoV is not delimited, reaching about 2π sr. Outside the imaging FoV, a rough location accuracy of a few tens of degrees can be obtained by exploiting the different offset of the two cameras and the detection plane architecture.

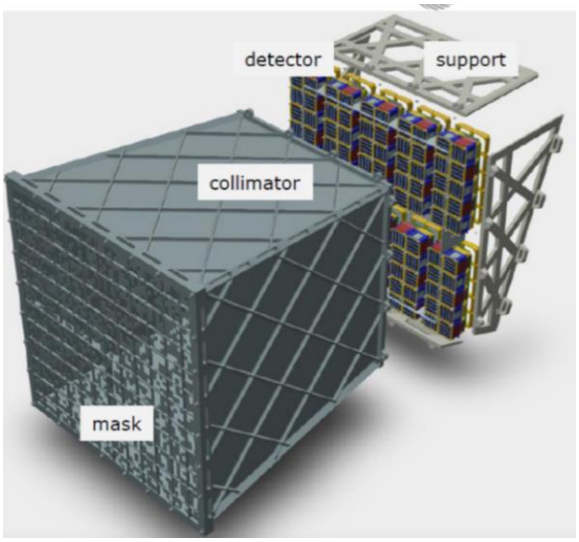

Figure 2. Exploded view of an XGIS camera.

Figure 2 shows a view of an XGIS camera that consists of the Collimator and Mask assemblies, made of W elements thick enough to be opaque to radiation up to 150 keV, the detector plane and the camera support and mechanical frame. A Cold-Finger for the detector thermal control is included. The XGIS detector plane contains 10×10 Modules arranged side by side. Each Module (Figure 3) contains 8×8 pixels (pitch 5 mm). A passive space, one pixel wide, interleaves one Module and the adjacent ones. In this way there are 9 "dead" rows and 9 "dead" columns in the plane. A Super-Module assembles 10 Modules, providing a mechanical structure to hold and align the Modules and the electrical Super-Module Back End Electronics (SM-BEE) with common services for the Modules. Finally, a Camera Back End Electronics board provides general logic, mass memory and interfaces to the DHU and the XSU (see the XGIS block diagram in Figure 4).

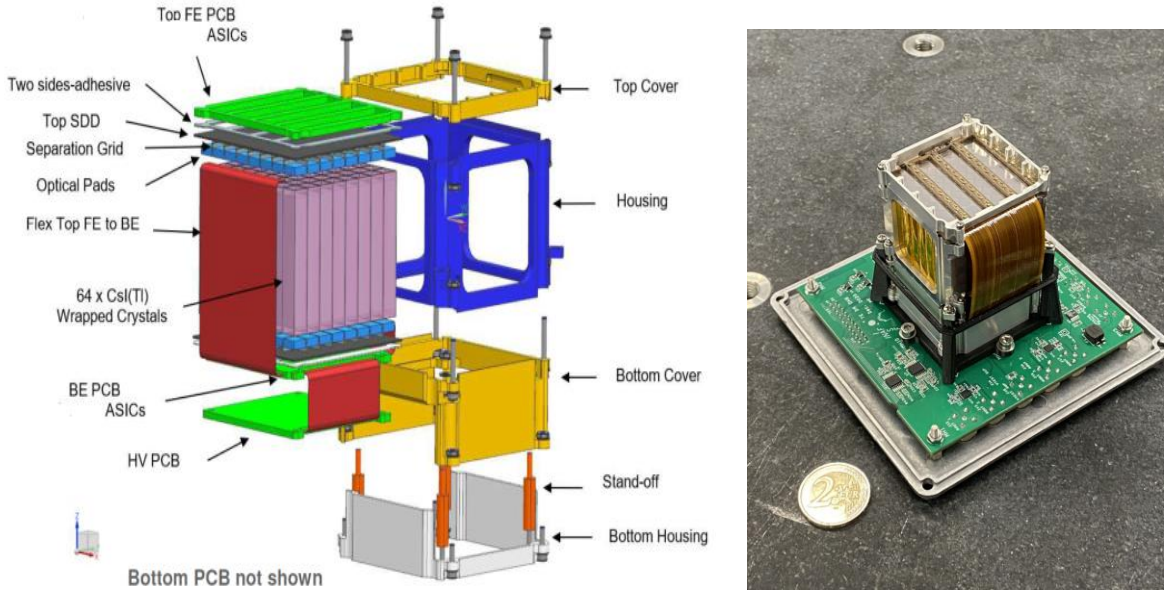

Figure 3. XGIS detector Module design (left) and full operating prototype (right) mounted on a test board.

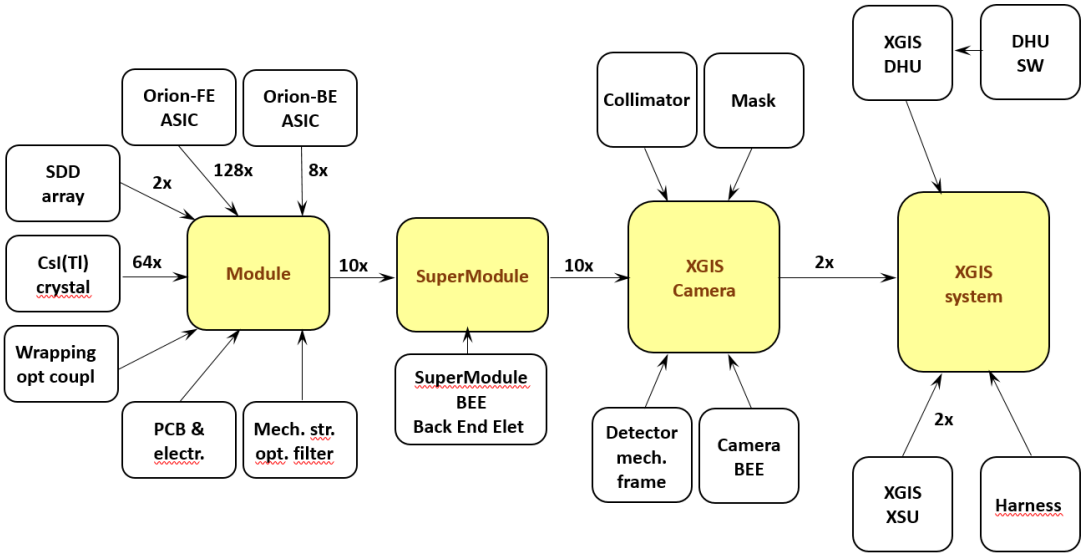

Figure 4. Block diagram of the XGIS system.

The Module is the basic element of the detector plane, it contains 64 autonomous pixels; the dedicated electronics can identify, convert in digital word and store all the information of a detected event. A view of a Module prototype realized during THESEUS ESA M5 activity is shown in Figure 3. It contains two Silicon Drift Detector (SDDs) chips arranged in an 8×8 array; between these, and coupled optically to them through transparent and flexible silicone pads, 64 CsI(Tl) scintillator bars (3 cm thick) are arranged. The crystal wrapping drives the light to the SDDs and optically insulates one crystal to the others. XGIS SDD have a square cross section 5×5 mm^2 while the scintillator crystal is 4.5×4.5×30 mm^3 in size. Top and bottom SDDs array are glued on a Printed Circuit Board (PCB), which hosts also the first stages of the electronic chain, the preamplifiers Front End ASIC, named Orion-FE[18]. A third PCB below, contains the ASICs Back End, named Orion-BE, that elaborates the Orion-FE signal and interfaces to SuperModule-BEE. The 'top PCB' has large openings to allow the incoming radiation to pass through and reach the active detecting elements, SDD and scintillator. An optical filter, not shown in Figure 3, will maintain dark operation condition for the SDD, while ensuring the maximum transparency for X-rays above 2 keV.

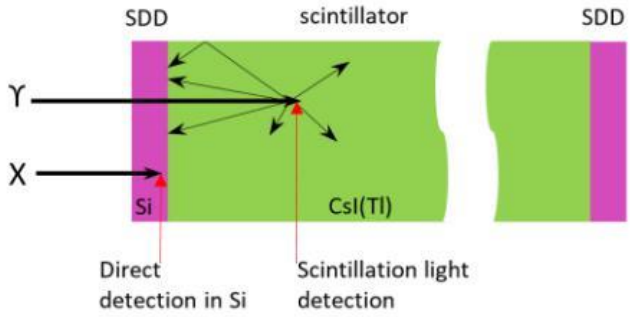

Figure 5. Pixel detector operation concept

Figure 5 shows the pixel operation concept. Two SDDs are placed at the two opposite sides of a scintillator CsI(Tl) crystal. Low energy radiation (roughly between 2 and 25–30 keV) is detected in the SDD on the top surface of the Module, while radiation with higher energy reaches the scintillator crystal. While the electron-hole pair creation from X-ray interaction in Silicon generates a fast signal (about 100 ns rise time), the scintillation light readout by SDD is dominated by the CsI(Tl) fluorescent states de-excitation time. As a consequence, scintillation and SDD signal should be integrated for different times to maintain the lowest noise and avoid significant ballistic deficit.

The discrimination between signals generated in Si (top SDD) and CsI(Tl) is done by the Orion-FE circuitry. The pixel size determines the position resolution in the detector plane for both direct SDD and scintillation detection. In the scintillator, the light is diffused/reflected on the crystal walls, and therefore attenuated, before reaching the SDDs. By weighing the two SDD signals (top and bottom) the scintillation depth in the bar can be evaluated producing a 3-D position detector.

A single channel Orion-FE ASIC is placed near each SDD anode, minimizing the stray capacitance and therefore the electronic noise, collects the SDD charge and performs a pre-amplification and buffering of the signal that is sent to the Orion-BE ASICs placed a few cm below. The signal processing in the Orion-BE (8 pixel) assumes that:

- An X-ray (2–30 keV) will be detected only in the top SDD, the best signal/noise ratio will be achieved with a short shaping time (typically 1 μs).
- An X-ray (>30 keV) will be detected in time coincidence in both top and bottom SDD; in this case the signal rise time will be of the order of few μs, due to the scintillation light characteristic timescale. The best signal/noise ratio will be achieved with a shaping time of the order of 3 μs typical.
- Three valid shaped signals (one short top two longer top and bottom) whose amplitude is above the noise, will be AD converted and digitally time marked inside Orion-BE ASIC.

- The digital signals from the Module's ASICs will be stored first in the Super-Module and in the Camera BEE, and then sent to the DHU where the data will be processed (see the XGIS DH-SW block diagram in Figure 6).

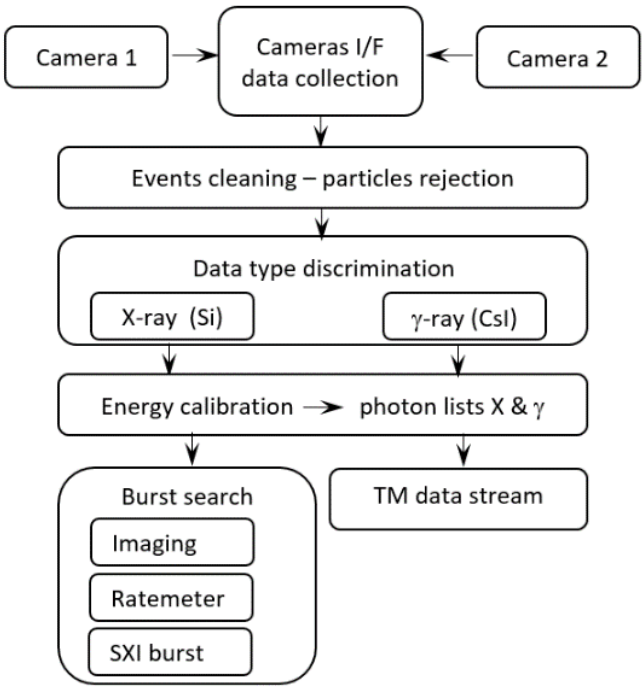

Figure 6. Block diagram of the XGIS DH SW

Here X and γ-events will be distinguished, and particle generated events will be discriminated on the basis of the energy deposit and topology of time coincident triggered pixels. Compton events can also be recognized. DHU will operate GRB search and triggering using essentially two methods based on rate and/or on images variations:

- The rate trigger method, which operates on the whole XGIS energy range, will compare variations of count rate in different energy bands, different integration times and different detector areas. Each estimated rate will be compared with the background rate evaluated dynamically.
- The image analysis operating up to 150 keV will compare images integrated on long time intervals (e.g. 20, 100, 500 s), and one or two energy ranges, with background images evaluated dynamically around the orbit with the same parameters. For each rate trigger event, the image analysis will be performed in order to get, in addition to the light curve, also the celestial direction of the event.

4. XGIS OPERATION, INTERFACES AND RESOURCES

XGIS operation modes, that follow THESEUS operational modes, are managed by the DHU as:

- Survey ("burst hunting") Mode: monitoring and looking, with different methods for GRBs within the FoV XGIS data will be partially in photon-by-photon mode and partially in time-integrated images and spectra.
- Burst Mode: in case a detected GRB, XGIS switches to the photon-by-photon mode.
- IRT Follow-up Mode: XGIS operates as in Survey Mode.

- External Trigger Mode: with a GRB observation triggered externally to THESEUS, trigger, XGIS will operate as in survey mode.
- IRT Observatory Mode: XGIS will operate as in Survey Mode

The data load in Gbit/orbit in one orbit for both XGIS cameras is shown in Table 3. It assumes an average background rate of about 6 events/cm^2/s, a burst average count rate of 10 events/cm^2/s, a burst lasting 1000 seconds with a follow up lasting 420 seconds, and 1 burst/orbit.

Table 2. XGIS data load foreseen for the different THESEUS modes.

	Imaging	**Gamma ph by ph**	**Total**
Survey mode	0.2	2.5	2.7
Follow up mode	-	0.3	0.3
Burst mode	-	3.6	3.6

The main physical parameters of the XGIS system are summarized in Table 3. The two Cameras are pointed at directions offset by +20° and –20° with respect to the S/C X-axis. The thermal interfaces with the S/C are a Cold Finger flange connecting the inside of the camera to the heat pipes coming from the spacecraft XGIS-radiator and the base of the Titanium support frame bolted to the payload platform. Overall, one camera must dissipate via radiative and conductive means about 50 W (without contingency). To maintain the temperature of the top SDD around 10 °C, to ensure their best performances, the Cold Finger should be maintained at 5 °C with the S/C platform at 20 °C. The main thermal interface of XSU and DHU boxes are their baseplate.

XGIS DHU provides instrument control for the two XGIS Camera units, as well as data processing, time management, instrument calibration, housekeeping (HK), and the switching of unregulated power. In detail:

•Data Interfaces: The XGIS DHU exchanges data, telecommands, and HK with the two Camera units via a single (cold-redundant) SpaceWire connection. The XGIS DHU interfaces with the S/C On-Board Digital Unit and Memory Management Unit (MMU) through a SVM-mounted SpaceWire Routing Switch. The DHU also receives PPS signals from the S/C through dedicated low-jitter lines. As the nominal Master DHU, the XGIS DHU also interfaces with the other I-DHUs. This is achieved by SpaceWire connections through the SpaceWire Router

•Power Interfaces: The XGIS DHU's receives an unregulated 28 V (TBC) from the S/C primary power line and passes them two XSUs. DHU is responsible for ON/OFF switching of the power.

Table 3. Size, mass and power budget of the XGIS system (without contingency).

	Camera (1 element)	**XSU (1 element)**	**DHU**	**Total (whole XGIS)**
Size [cm]	@ base level 50 × 56.6 @ mask level 60 × 60 Height 91.8	35 × 22 × 12	21 × 21 × 13	
Mass [kg]	66 + 2 (Harness)	8	7	159
Power [W]	50	29	15	173

5. EXPECTED PERFORMANCES

The main expected performances of the XGIS[16,19] are summarized in Table 4. The XGIS response as a function of photon energy and off-axis angle were derived from Monte-Carlo simulations making use of instrument and spacecraft GEANT4 mass models[16]. The particle-induced background level, spectrum and orbital modulation (outside the South Atlantic Anomaly, SAA) were evaluated by combining these models with the predictions of the ESA-validated trapped proton radiation models for the foreseen altitude and inclination of the THESEUS orbit[16].

Table 4. XGIS main scientific performance characteristics.

Energy Range	**2 – 150 keV**	**150 keV – 10 MeV**
Field of View	~2sr (imaging, PC)	~6sr
Peak eff. area	~500 cm^2	~1000 cm^2
Sensitivity **(5σ , 1s)**	~10^{-8} cgs in 2–30 keV ~$3x10^{-8}$ cgs in 30–150 keV	~$3x10^{-7}$ cgs in 150 keV – 1 MeV
Angular resolution	<120 arcmin	
Source location accuracy	≤ 15 arcmin 90% c.l. in 2-150 keV (SNR > 7)	>10° (exploiting cameras geometry and misalignment)
Timing accuracy	~7 μs	~7 μs
Energy resolution	≤ 1200 eV FWHM @ 6 keV	≤ 6 % FWHM @ 500 keV

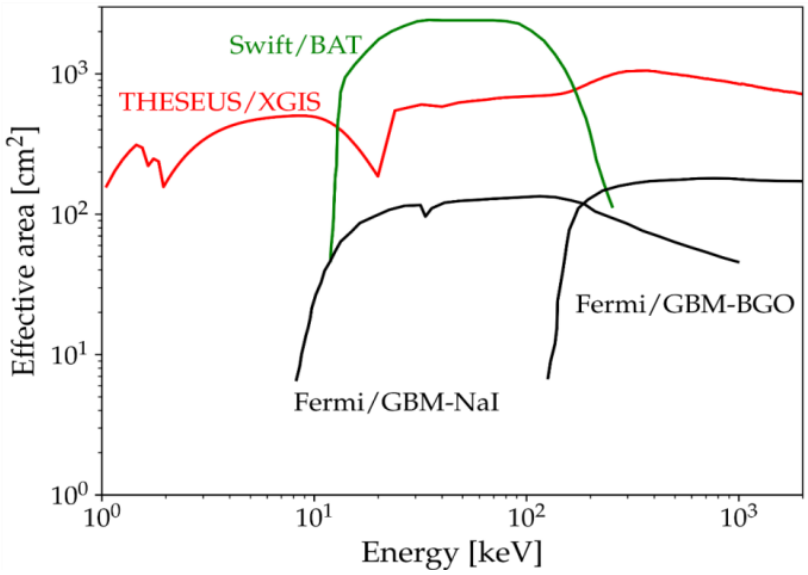

Figure 7. Peak effective are of the XGIS as a function of energy, comparted to that of Swift/BAT and Fermi/GBM.

Figure 7 shows the XGIS peak effective area as a function of photon energy, compared to those of some of the main GRB detectors currently operating. As can be seen, the XGIS shows an unprecedented combination of effective area and energy band, allowing the detection, accurate location and spectral / timing characterization of all classes of GRBs (high-redshift, under-luminous, ultra-long, classic long and short ones, peculiar short ones like the GRB/GW event of August 17, 2017) and other classes of bright X-ray transients.

The expected XGIS on-axis sensitivity as a function of exposure for different source power-law spectra is shown in the left panel of Figure 8, whereas the right panel of the same figure shows the source location accuracy as a function of exposure and for different off-axis angles and assuming a source with 500 mCrab flux in the 2 – 150 keV energy range[19].

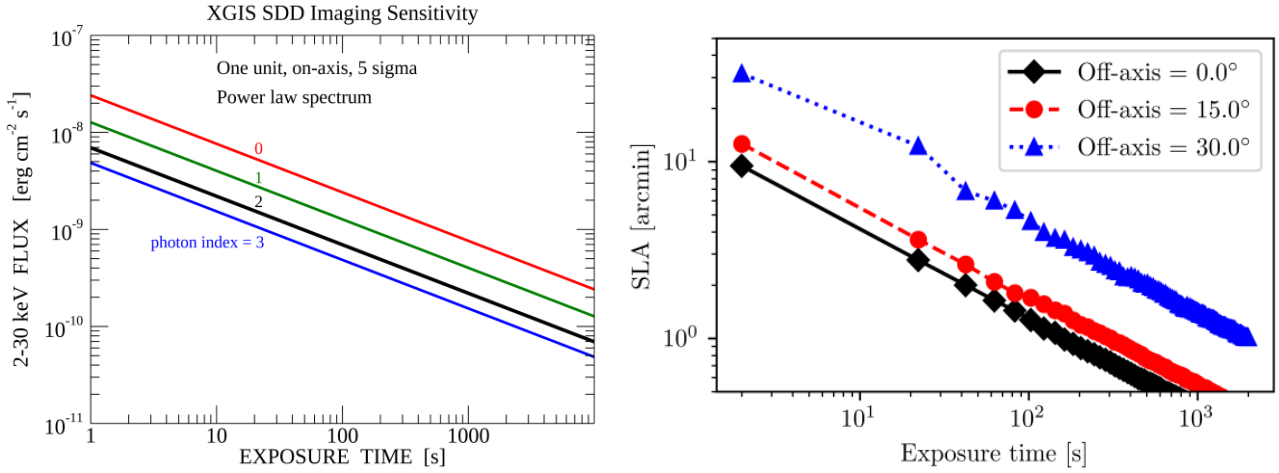

Figure 8. Left: XGIS imaging sensitivity (5σ confidence level) as a function of exposure time provided by the SDDs in the 2-30 keV range for a single XGIS unit and sources in the fully coded field of view (the central 10x10 deg^2 of each unit's FoV). The different lines refer to sources with a power law spectrum with the indicated photon index. By combining the two units, the sensitivity plotted here is achieved over a 60x30 deg^2,Right: XGIS Source Location Accuracy (SLA) as a function of exposure for a 500 mCrab source detected at different offset angles.

As mentioned in previous sections, during the Phase A study as candidate M5, ESA, together with the Consortium, developed a sophisticated Mission Observation Simulator (MOS), which allowed to assess in a most reliable way the expected detection rates of different type of events by the three scientific instruments. The MOS software included, for each instrument, the FoV, the Field of Regard (FoR), the expected response (as a function of source intensity, off-axis, spectrum, detection algorithms, etc.), background level and modulation, thermal control, stray-light, Earth, Sun and Moon avoidance angles, and other constraining factors, as well all operation constraints of the spacecraft itself[3]. For the XGIS, in addition to the above, the detection ("trigger") sensitivity to GRB included the identification and simulation of sophisticated trigger algorithms[19,20] , tested on simulated and real (form current main GRB detectors) images and light curves. Intensive simulations of the satellite operating in LEO with 4 degrees inclination and different pointing strategies were performed by assuming a nominal duration of scientific operations of 3.5 years, thus allowing to assess the compliance of instruments and mission profile with the scientific requirements and optimizing the instruments and mission design as well as the scientific operation concept.

In Table 5, we report the expected average XGIS detection rates in its imaging FoV (~2sr, location accuracy <15 arcmin), as derived from the MOS, including total long and short GRB rates, high-z GRB rates, and expected simultaneous detections with a third generation GW detector like Einstein Telescope (ET)[3,5,6,21].

Table 5. XGIS detection rates in its imaging FoV for different classes of GRBs based on ESA/M5 Phase A study Mission Observation Simulator.

GRB type	**Detections in 3.5 years**
Long	~ 1000
Long at z>6	~ 65
Short (imaging FoV)	~ 42
Short (total FoV)	~ 75
Short with GW counterpart (ET)	~25 - 35

6. MATURITY AND PERSPECTIVES

Due to the modularity of XGIS, its detector module is the key technological element of the system; its most critical components such as the SDD and the ASICs, as well the module mechanical design assembly, were significantly developed during the ESA/M5 Phase-A study of THESEUS. SDDs have been used in many experiments on ground, and proposed for space mission such as eXTP[22] and the nano-satellite constellation HERMES[23]. Their heritage came from the long lasting (about 15 years) ReDSoX collaboration, where many iterations in the SDD design were performed by INFN (Istituto Nazionale di Fisica Nucleare) and produced by FBK "Fondazione Bruno Kessler", including the full SDD 64 element XGIS SDD-array. Within the ReDSoX collaboration, the expertise from Polytechnic of Milan and University of Pavia, allowed the successful development of several mixed-signal ASICs. For THESEUS the ORION ASICs were already realized and tested[18]. SDD and ASIC production was funded by ASI during THESEUS M5. In the same period ESA funded the activity to realize and test a complete module prototype with the aim of testing the whole mechanical design (see Figure 3) that include all the final elements of the module except for the ORION ASIC, then not yet available, replaced by the LYRA ASIC, from the HERMES project, based on the same philosophy but with reduced electrical characteristics. XGIS improvements will certainly include the realization of a module with the ORION ASIC. The possibility to use a more performant scintillator material such as the recently developed GAGG(Ce) (already used in HERMES) will be also evaluated.

R&D activities during THESEUS Phase A Study as ESA/M5 candidate allowed to reach a TRL of at least 4 for the ASIC and 5 for the SDD+CsI detection elements (with identified path for reaching TRL 6 by 2024). TDA study by OHB-I and INAF-OAS, funded by ESA, was dedicated to define requirements, to design, manufacture, and test a XGIS Detection Module (DM) prototype; achieved maturity level of TRL 4/5. In order to obtain a TRL6, the XGIS DM would need a more robust mechanical design able to withstand the launch loads and the use of a new ASIC component of the Orion family[18], designed and produced specifically for the XGIS and currently under testing. Study of Alternative DM concepts with larger sub-array dimensions and a smaller pixel size to improve spatial resolution and provide polarimetric capabilities

In conclusion, we remark that an XGIS-like instrument will improve substantially the capability of future missions for multi-messenger astrophysics and GRB science. In this respect, the modularity of the design grants great flexibility in adapting the XGIS configuration for specific scientific objectives and available resources (e.g., inclusion in the payload of a medium / large mission or a dedicated "stand-alone" small satellite). In addition, as described above, the ESA Phase A study of THESEUS and related TDAs grant an already good TRL level (e.g., detection module prototype, SDD detectors and specifically designed ASIC already under testing). Preliminary MC simulations have already demonstrated the possibility of extended capabilities by exploiting 3D detection plane for performing Compton polarimetry and providing source location outside imaging FoV.

REFERENCES

[1] Amati, L., O'Brien, P., Gotz, D., Bozzo, E., Tenzer, C., et al., "The THESEUS space mission concept: science case, design and expected performances", Advances in Space Research, 62, 1, 191 (2018).

[2] Amati, L, O'Brien, P., Gotz, D., Bozzo, E., Santangelo, A., et al., "The THESEUS space mission: science goals, requirements and mission concept", Experimental Astronomy, 52, 3, 183 (2021).

[3] ESA, "THESEUS Assessment Study Report (Yellow Book)", ESA/SCI(2021)2 (2021).

[4] Tanvir, N.R., Le Floc'h, E, Christensen, L., Caruana, J., Salvaterra, R., et al., "Exploration of the high-redshift universe enabled by THESEUS", Experimental Astronomy, 52, 3, 219 (2021).

[5] Stratta, L., Ciolfi, R., Amati, L., Bozzo, E., Ghirlanda, G:, et al., "THESEUS: A key space mission concept for Multi-Messenger Astrophysics", Advances in Space Research, 62, 3, 662 (2018).

[6] Ciolfi, R., Stratta, G., Branchesi, M., Gendre, B., Grimm, S., et al., "Multi-messenger astrophysics with THESEUS in the 2030s", Experimental Astronomy, 52, 3, 245 (2021).

[7] Mereghetti, S., Balman, S., Caballero-Garcia, M., Del Santo, M., Doroshenko, V., et al., "Time domain astronomy with the THESEUS satellite", Experimental Astronomy, 52, 3, 309 (2021).

[8] Ghirlanda, G., Salvaterra, R., Toffano, M., Ronchini, S., Guidorzi, C., et al., "Gamma ray burst studies with THESEUS", Experimental Astronomy, 52, 3, 277 (2021).

[9] Burderi, L., Sanna, A., Di Salvo, T., Riggio, A., Iaria, R., et al., "Quantum gravity with THESEUS", Experimental Astronomy, 52, 3, 439 (2021).

[10] Rosati, P., Basa, S., Blain, A.W., Bozzo, E., Branchesi, M., et al., "Synergies of THESEUS with the large facilities of the 2030s and guest observer opportunities", Experimental Astronomy, 52, 3, 407 (2021).

[11] Piro, L., Ahlers, M., Coleiro, A., Colpi, M., de Oña Wilhelmi, E., et al., "Multi-messenger-Athena Synergy White Paper", in press on Experimental Astronomy, eprint arXiv:2110.15677 (2021).

[12] O'Brien, P., Hutchinson, I., Lerman, H., Feldman, C., McHugh, M., et al., "The soft x-ray imager on THESEUS: the transient high energy survey and early universe surveyor", Proceedings of the SPIE, Volume 11444, id. 114442L (2020).

[13] Labanti, C., Amati, L., Frontera, F., Mereghetti, S:, Gasent-Blesa, J.L., et al., "The X/Gamma-ray Imaging Spectrometer (XGIS) on-board THESEUS: design, main characteristics, and concept of operation", Proceedings of the SPIE, Volume 11444, id. 114442K (2020).

[14] Gotz, D., Basa, S., Pinsard, F., Martin, L., Arhancet, A., et al., "The Infra-Red Telescope (IRT) on board the THESEUS mission", Proceedings of the SPIE, Volume 11444, id. 114442M (2020).

[15] Gasent-Blesa, J.L., Reglero, V., Connell, P., Pinazo-Herrero, B., Navarro-Gonzaléz, J., et al., "The XGIS imaging system onboard the THESEUS mission", Proceedings of the SPIE, Volume 11444, id. 114448S 16 pp. (2020).

[16] Campana, R., Fuschino, F., Labanti, C., Mereghetti, S., Virgilli, E, et al., "The XGIS instrument on-board THESEUS: Monte Carlo simulations for response, background, and sensitivity", Proceedings of the SPIE, Volume 11444, 114448P (2020).

[17] Fuschino, F., Campana, R., Labanti, C., Amati, L., Virgilli, E., et al., "The XGIS instrument on-board THESEUS: the detection plane and on-board electronics", Proceedings of the SPIE, Volume 11444, id. 114448R 14 pp. (2020).

[18] Mele, F., Dedolli, I., Gandola, M., Grassi, M., Malcovati, P., et al., "ORION, a Multichip Readout Electronics for Satellite Wide Energy Range X-/γ-Ray Imaging Spectroscopy: Design and Characterization of the Analog Section", IEEE Transactions on Nuclear Science, vol. 68, issue 12, pp. 2801-2809 (2021).

[19] Mereghetti, S., Ghirlanda, G., Salvaterra, R., Campana, R:, Labanti, C., et al., "Proceedings of the SPIE, Volume 11444, id. 114448R 14 pp. (2020).

[20] Guidorzi, C., "MEPSA: A flexible peak search algorithm designed for uniformly spaced time series", MEPSA: A flexible peak search algorithm designed for uniformly spaced time series (2015).

[21] Ronchini, S., Branchesi, M., Oganesyan, G., Banerjee, B., Dupletsa, U., "Perspectives for multi-messenger astronomy with the next generation of gravitational-wave detectors and high-energy satellites", arXiv, 2204.01746 (2022).

[22] Zhang, S.N., Feroci, M., Santangelo, A., Dong, Y.W., Feng, H., wt al., "eXTP: Enhanced X-ray Timing and Polarization mission", Proceedings of the SPIE, Volume 9905, id. 99051Q 16 pp. (2016).

[23] Fiore, F., Burderi, L., Lavagna, M., Bertacin, R., Evangelista, Y., et al., "The HERMES-technologic and scientific pathfinder", Proceedings of the SPIE, Volume 11444, id. 114441R 15 pp. (2020).